

Skeletal mineralization defects in adult hypophosphatasia—a clinical and histological analysis

F. Barvencik · F. Timo Beil · M. Gebauer · B. Busse ·
T. Koehne · S. Seitz · J. Zustin · P. Pogoda · T. Schinke ·
M. Amling

Received: 14 April 2010 / Accepted: 3 January 2011

© International Osteoporosis Foundation and National Osteoporosis Foundation 2011

Abstract

Summary Histomorphometry and quantitative backscattered electron microscopy of iliac crest biopsies from patients with adult hypophosphatasia not only confirmed the expected enrichment of non-mineralized osteoid, but also demonstrated an altered trabecular microarchitecture, an increased number of osteoblasts, and an impaired calcium distribution within the mineralized bone matrix.

Introduction Adult hypophosphatasia is an inherited disorder of bone metabolism caused by inactivating mutations of the

ALPL gene, encoding tissue non-specific alkaline phosphatase. While it is commonly accepted that the increased fracture risk of the patients is the consequence of osteomalacia, there are only few studies describing a complete histomorphometric analysis of bone biopsies from affected individuals. Therefore, we analyzed iliac crest biopsies from eight patients and set them in direct comparison to biopsies from healthy donors or from individuals with other types of osteomalacia.

Methods Histomorphometric analysis was performed on non-decalcified sections stained either after von Kossa/van Gieson or with toluidine blue. Bone mineral density distribution was quantified by backscattered electron microscopy.

Results Besides the well-documented enrichment of non-mineralized bone matrix in individuals suffering from adult hypophosphatasia, our histomorphometric analysis revealed alterations of the trabecular microarchitecture and an increased number of osteoblasts compared to healthy controls or to individuals with other types of osteomalacia. Moreover, the analysis of the mineralized bone matrix revealed significantly decreased calcium content in patients with adult hypophosphatasia.

Conclusions Taken together, our data show that adult hypophosphatasia does not solely result in an enrichment of osteoid, but also in a considerable degradation of bone quality, which might contribute to the increased fracture risk of the affected individuals.

Keywords Alkaline phosphatase · Histomorphometry · Osteoid · Osteomalacia · qBEI

Florian Barvencik and Frank Timo Beil contributed equally to this work and therefore share first authorship.

F. Barvencik · F. T. Beil · M. Gebauer · B. Busse · T. Koehne ·
S. Seitz · P. Pogoda · T. Schinke · M. Amling (✉)
Department of Osteology and Biomechanics,
University Medical Center Hamburg-Eppendorf,
Martinistrasse 52,
20246, Hamburg, Germany
e-mail: amling@uke.uni-hamburg.de

F. T. Beil · S. Seitz
Department of Orthopaedics,
University Medical Center Hamburg-Eppendorf,
Hamburg, Germany

B. Busse
Materials Sciences Division, Lawrence Berkeley National
Laboratory, University of California,
Berkeley, USA

J. Zustin
Institute of Bone Pathology,
University Medical Center Hamburg-Eppendorf,
Hamburg, Germany

P. Pogoda
Department of Trauma-, Hand- and Reconstructive Surgery,
University Medical Center Hamburg-Eppendorf,
Hamburg, Germany

which is caused by inactivating mutations of the gene *ALPL*, encoding the tissue non-specific alkaline phosphatase [1–9]. Depending on the type of mutation and the mode of inheritance, the disease is highly variable in its clinical expression and can be classified into six major forms (perinatal lethal, prenatal benign, infantile, childhood, adult, and odontohypophosphatasia) [10]. Given the severe skeletal hypomineralization, the perinatal form either results in stillbirth or in early postnatal lethality [11, 12]. The clinical course of the infantile form starts in the first 6 months of life and is characterized by rickets, craniosynostosis, nephrocalcinosis, and premature death [13]. After the first year, the childhood form of hypophosphatasia is characterized by short stature, bone deformities of the lower extremities, and premature loss of primary teeth [13, 14]. The adult form of hypophosphatasia is mainly characterized by osteomalacia, pseudofractures, and pathologic fractures after minimal trauma, as well as by muscle and joint pain [15–18].

The clinical diagnosis of hypophosphatasia is, however, not only based on radiological findings or bone mineral density (BMD) measurements, but also on biochemical assays, such as monitoring the serum activities of alkaline phosphatase, which are reduced in the affected individuals. In addition, elevated levels of phosphoethanolamine in the urine or of pyridoxal-5-phosphate in the serum are supporting the diagnosis of hypophosphatasia, since these substrates of alkaline phosphatase accumulate in the absence of the enzyme [19]. Moreover, the genetic screening methods that are available nowadays have led to the identification of more than 221 mutations of the *ALPL* gene so far and have helped in the understanding of the genetic causes underlying the variability of clinical expression [20]. These methods have not only allowed the performance of prenatal diagnostics of the disease, but also helped to confirm the diagnosis of hypophosphatasia [19]. However, while there is no doubt about the usefulness of genetic diagnosis in the case of hypophosphatasia, the availability of these methods certainly explains why histopathological analyses of bone biopsies from affected individuals are not routinely performed anymore.

In fact, the largest histologic study so far, describing skeletal pathologies in various forms of hypophosphatasia, was published in 1984 [21]. Through the use of non-decalcified sections from iliac crest biopsies, the authors were able to demonstrate an enrichment of osteoid in most of the affected individuals, whose degree reflected the clinical severity of the disease. From the 17 cases of adult hypophosphatasia analyzed in this study, 11 were diagnosed with osteomalacia, while five others were characterized by decreased bone remodeling. Taken together, these and other data have helped in the understanding of the skeletal manifestations of hypophosphatasia [22–26]. However,

since there are no larger studies being performed after the standardization of bone histomorphometry by the American Society for Bone and Mineral Research [27], we decided to analyze iliac crest biopsies from eight individuals suffering from adult hypophosphatasia using non-decalcified histology, which were compared to biopsies from age-matched individuals without skeletal abnormalities or to biopsies from individuals with other types of osteomalacia. In addition, we have applied quantitative backscattered electron microscopy to determine the calcium distribution within the mineralized bone matrix.

Methods

Patients and histological analysis of iliac crest biopsies

In this study, we included eight adult hypophosphatasia patients from whom iliac crest bone biopsies were assessed in the bone pathology department of the University Medical Center Hamburg-Eppendorf. All patient records were screened, and the relevant clinical data were extracted. The group included six women and two men between 24 and 66 years of age (average age of 47 years, average height of 168 cm). Eight age- and sex-matched cases from our iliac crest archive without any bone disease were integrated in this study as a control group (six females and two males, average age of 48 years). All of these individuals died in accidents or of acute disease. Reviews of hospital records and autopsy reports were used to exclude individuals with cancer, diabetes, glucocorticoid medication, or donors on other drugs known to affect calcium metabolism. Moreover, patients with severe liver or kidney disease or periods of longer immobilization before biopsy were excluded. In addition, we have analyzed biopsies from eight individuals with low circulating 25 (OH)-vitamin D levels (8.8 ± 3.3 ng/ml), with an average age of 49 years, and from one patient suffering from X-linked hypophosphatemic rickets (male, 45 years old). This study was carried out according to existing rules and regulations of the University Medical Center Hamburg-Eppendorf and is in line with the “Hamburg Hospital Law (HmbKHG) April 17th, 1991: Patient Security §12.”

Non-decalcified histology

As previously described by Bordier, all samples from the iliac crest were dissected out 2 cm below and 2 cm behind the crista iliaca superior anterior and fixed overnight at 4°C in 3.7% PBS-buffered formaldehyde [28]. After dehydration in ascending concentrations of ethanol, the samples were embedded non-decalcified in methylmethacrylate, and 5- μ m-thick sections were cut using a Microtec rotation

microtome (Techno-Med; Munich, Germany). The sections were stained according to standard protocols after von Kossa/van Gieson, Goldner, or with toluidine blue as described [29–32].

Dual-energy X-ray absorptiometry

BMD was measured by dual-energy X-ray absorptiometry (DXA) (Lunar Prodigy en Core 2007, GE Healthcare; Madison, WI, USA). Two skeletal areas, the left proximal femur and the lumbar spine (L1–L4), were evaluated by DXA. The patients were scanned according to the manual supplied by the manufacturer and were placed in the supine position. The detected BMD of the projected bone area was expressed in grams per square centimeter (g/cm^2), and the corresponding T-Score was calculated.

Quantitative histomorphometry

Parameters of static histomorphometry were quantified on toluidine blue–or von Kossa/van Gieson-stained non-decalcified sections of iliac crest biopsies. Analyses of bone volume (BV/TV), trabecular thickness (Tb.Th), trabecular number (Tb.N), trabecular separation (Tb.Sp), osteoid volume (OV/BV), osteoid surface (OS/BS), as well as the determination of osteoblast (N.Ob/B.Pm), osteoclast number (N.Oc/B.Pm), osteocyte number (Ot.N/B.Ar/ mm^2) and surface indices (Ob.S/BS and Oc.S/BS), mineralized bone volume (Md.V/TV), and osteoclasts surface per mineralized bone surface (Oc.S/Md.BS) were carried out according to the ASBMR standards using the Osteo-Measure histomorphometry system (Osteometrics; Atlanta, GA, USA) connected to a Zeiss microscope (Carl Zeiss; Jena, Germany) [27]. We did not perform dynamic histomorphometry in our study.

Bone mineral density distribution measurements by quantitative backscattered electron imaging

BMD distribution (BMDD) measurements were performed on non-decalcified, coplanar polished, carbon-coated methylmethacrylate-embedded bone biopsies. The technical application is based on the work of other groups using qBEI and has been reported previously [33–38]. The scanning electron microscope (LEO 435 VP; Cambridge, England) was operated at 15 kV and 665 pA at a constant working distance (BSE Detector, type 202, K.E. Developments Ltd.; Cambridge, England). The pixel size amounts to 3 μm and lies within the recommendation range of Roschger et al. [34]. The standardization of the method was accomplished by the analysis of synthetic hydroxyapatite (HA). Seven HA samples with increasing Ca/P ratios (D.O. T. Medical Solutions; Rostock, Germany) were evaluated

with energy dispersive X-ray analysis and qBEI to create a calibration curve. A highly linear relationship between backscattered electron imaging gray values and the calcium content (Ca-wt.%) has been reported previously by other authors [34, 36, 39]. The linear dependence ($R^2=0.98$) of the evaluated HA gray values due to the respective calcium concentration of the HA samples enables the calibration of the method.

Statistical analysis

All data are presented as means \pm SD. Statistical analysis of histomorphometric values was compared using unpaired Student's *t* test. Statistical differences were considered significant when $p < 0.05$.

Results

Clinical diagnosis of hypophosphatasia

Diagnosis of adult hypophosphatasia was based on characteristic clinical and laboratory findings. Pain and discomfort in the thighs and hips were often present, and pseudofractures (Looser Zones), for example of the femur, fibula, or tibia, could be verified on plain X-ray films (Fig. 1a, c, f). Also bone deformities, which occur with this disease, like pathologic alteration of the joint axis (Fig. 1c) and bowing of the femur (Fig. 1d), were documented on radiographs. In addition, we observed pathologic calcium accumulation in other organs by ultrasound, especially in the kidney (Fig. 1g). DXA performed in the femur and lumbar spine demonstrated low BMDs in adult hypophosphatasia patients (Fig. 1e).

Biochemical analysis of serum, plasma, and urine demonstrated reduced levels of alkaline phosphatase (AP) (27.8 ± 4.5 U/l; normal range, 35–104 U/l), bone-specific alkaline phosphatase (BAP) (5.0 ± 1.4 $\mu\text{g}/\text{l}$; normal range, 6–26 $\mu\text{g}/\text{l}$) and elevated levels of pyridoxal phosphate (PLP) (41.2 ± 14.4 ; normal range, 7.5–18.5 $\mu\text{g}/\text{l}$). In contrast, serum levels of phosphate, calcium, 25-OH vitamin D₃, intact parathyroid hormone (PTH), and creatinine were in the normal range, which ruled out the existence of secondary hyperparathyroidism (Fig. 1e). Pregnancy, anemia, hypothyroidosis, anorexia, and malnutrition that can also cause decreased alkaline phosphatase levels were ruled out by clinical and laboratory examinations.

Histological findings

The light microscopic findings of the iliac crest bone biopsies revealed distinct differences between hypophosphatasia patients and control individuals. The von Kossa/van Gieson- or Goldner-stained specimens of the control

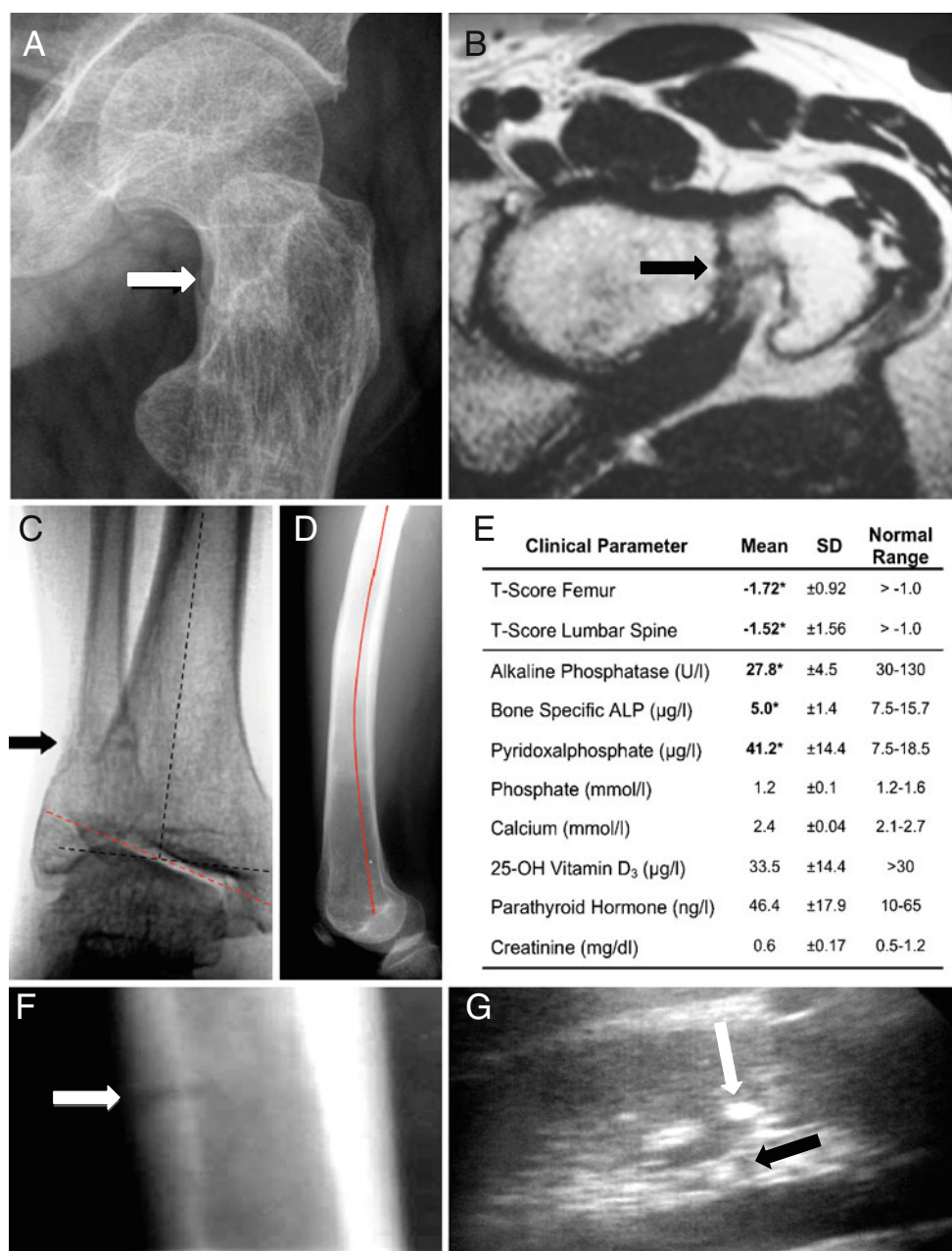


Fig. 1 Typical clinical aspects of adult hypophosphatasia. **a** X-ray (oblique view) and **b** MRI (axial view) of the left lateral proximal femur of a 32-year-old male patient diagnosed with adult hypophosphatasia. A pseudo-fracture in the femoral neck is indicated by the arrow. **c** X-ray (a.p. view) of the right ankle joint of the same patient showing also a pseudo-fracture in the distal fibula. In addition, a pathologic tilt of the ankle joint axis was observed (dotted red line, pathologic axis; dotted black line, anatomic axis). **d** The pronounced

bowing of the left femur (red line) is clearly visible by X-ray (lateral view). **e** Results of bone densitometry and biochemical analysis. The normal ranges of all parameters are given on the right. Pathological abnormalities in the hypophosphatasia patients ($n=8$) are highlighted in boldface. **f** X-ray (lateral view) of the tibia showing a pseudo-fracture of the tibial shaft (white arrow). **g** Ultrasound of the kidney illustrating a calcification spot as an echogenic focus (white arrow) with posterior acoustic shadowing (black arrow)

group showed a normal orientation and distribution of the trabeculae in the cancellous bone, with only thin layers of osteoid (Fig. 2a, b). Compared to the control group, the iliac crest biopsies of the hypophosphatasia patients were remarkably different with increased osteoid volume (Fig. 2a, b). In the toluidine blue-stained sections, the

outline of the trabeculae seemed to be regularly formed, but the impaired mineralization in hypophosphatasia patients resulted in an irregularly formed mineralized part of trabeculae lying underneath the thick osteoid layer (Fig. 2c). In fact, the interface between mineralized bone and unmineralized osteoid was irregularly shaped in

Fig. 2 Non-decalcified histology of iliac crest biopsies from healthy individuals and adult hypophosphatasia patients. **a** von Kossa/van Gieson staining ($\times 25$ magnification) and **b** Goldner staining ($\times 100$ magnification) showing an accumulation of osteoid (stained in red) in hypophosphatasia patients. The red arrow indicates a site where a complete trabecule is bridged by osteoid. **c** Toluidine blue staining ($\times 400$ magnification) confirms the existence of thick osteoid layers (red arrows) in hypophosphatasia patients and demonstrated an increased number of osteoblasts covering these surfaces. The white arrows indicate scalloped appearance of the cement lines, which were characteristic for the hypophosphatasia cases. **d** Polarized brightfield microscopy reveals an accumulation of osteoid (red arrows) but also demonstrates that the lamellar structures observed in control biopsies (white arrows) are impaired in the hypophosphatasia cases. The insert shows basophilic pellets accumulating on the osteoid, which was also characteristic for the sections of the hypophosphatasia patients

sections from hypophosphatasia patients, which resembles the findings reported by Balena et al., who has introduced the term “scalloped cement lines” [40].

At the cellular level, both osteoclasts and osteoblasts appeared morphologically similar in the two groups. However, toluidine-blue staining revealed an increased number of osteoblasts in the hypophosphatasia patients, which were orientated in line on the thick layer of osteoid (Fig. 2c). Moreover, a polarized microscopic view revealed striking differences between the two groups. In fact, the regular structure of bone layers is disrupted in hypophosphatasia patients by areas of unmineralized osteoid that seem to be randomly distributed (Fig. 2d). At the interface of osteoid and mineralized bone, we further observed basophilic pellets, which may represent clusters of calcium complexes (Fig. 2d). Interestingly, these structures did not progress uniformly outward from the cement line, thus implying that the deficiency of *ALPL* rather affects the initiation of mineralization, rather than its continuation.

Quantitative histomorphometry

To quantify the observed structural changes, we performed histomorphometry according to the guidelines of the American Society for Bone and Mineral Research (Table 1). We first determined the trabecular bone volume (BV/TV) and found a non-significant increase in the biopsies derived from the hypophosphatasia patients compared to the control group. In addition, we observed a significant increase of the trabecular number (Tb.N) and a significant decrease of trabecular separation (Tb.Sp) and thickness (Tb.Th) in sections from hypophosphatasia patients. As expected, the biopsies from hypophosphatasia patients also showed a significant increase in osteoid volume (OV/BV) and osteoid surface (OS/BS) compared to biopsies taken from the control group. Therefore, when we determined the mineralized bone volume per tissue volume (Md.V/TV), there was no increase in the hypophosphatasia cases.

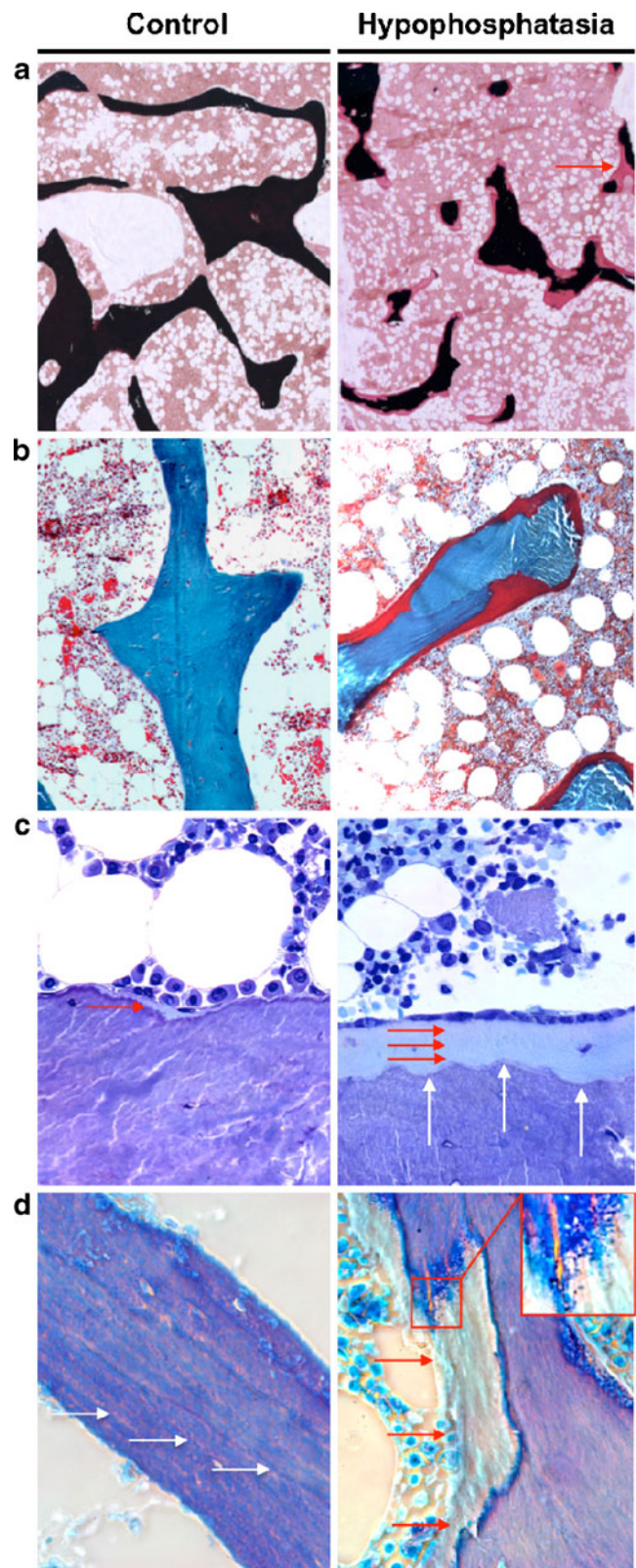


Table 1 Histomorphometric parameters of the iliac crest biopsies derived from healthy donors (control) and adult hypophosphatasia patients (HP)

Parameter	Control	SD	HP	SD	<i>P</i> value
BV/TV (%)	19.5	±7.1	24.0	±5.7	0.06
Tb.Th (μm)	164.1	±53.2	118.5	±16.6	0.04*
Tb.N (mm ⁻¹)	1.21	±0.3	2.19	±0.4	0.01*
Tb.Sp (μm)	738.0	±336.9	351.2	±88.1	0.01*
OV/BV (%)	0.95	±0.9	16.2	±14.3	0.01*
OS/BS (%)	6.5	±6.0	47.8	±19.3	0.01*
O.Th (μm)	3.9	±2.2	16.4	±9.7	0.01*
N.Ob/B.Pm (mm ⁻¹)	2.4	±0.6	4.1	±1.4	0.01*
Ob.S/BS (%)	2.8	±1.1	6.2	±2.1	0.01*
N.Oc/B.Pm (mm ⁻¹)	0.10	±0.1	0.13	±0.1	0.54
Oc.S/BS (%)	0.43	±0.4	0.45	±0.3	0.93
N.Ot/B.Ar (/mm ²)	120.1	±16.7	119.7	±15.8	0.96
Md.BV/TV (%)	19.3	±7.1	22.2	±6.6	0.40
N.Oc/Md.BS (mm ⁻¹)	0.45	±0.4	1.9	±2.4	0.11

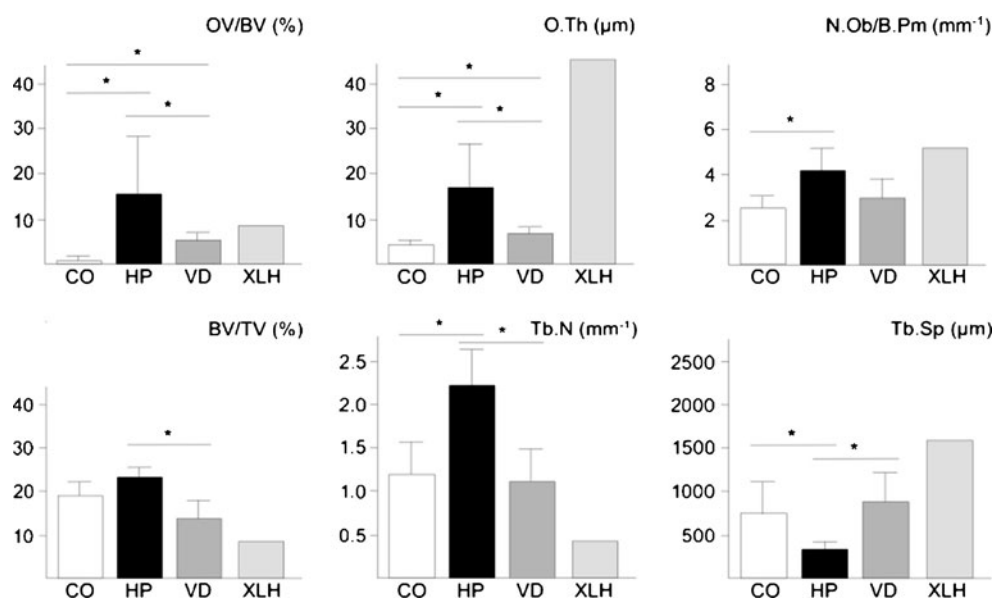
Shown are the mean values and standard deviation (SD)

* *P* values below 0.05 were considered statistically significant

We next quantified the numbers of osteoblasts, osteoclasts, and osteocytes. Here we found an increase of osteoblast number (N.Ob/B.Pm) and surface (Ob.S/BS) in the hypophosphatasia patients, although their morphology appeared to be normal. In contrast, the number (N.Oc/B.Pm) and surface of osteoclasts (Oc.S/BS) were not significantly different between the two groups, and the same was the case for the osteocyte number (Ot.N/B.Ar/mm²). Given the large increase of the osteoid surface in the cases of adult hypophosphatasia, we further quantified the osteoclast surface per mineralized bone surface (Oc.S/MS). Here we observed a non-significant increase compared to the control cases, which may explain, at least in part, the scalloped pattern of cement lines described above.

To address the question, whether the increased osteoblast number and the structural changes of trabecular bone are generally observed in cases of osteomalacia, we further performed histomorphometry in biopsies derived from eight individuals with low circulating 25 (OH)-vitamin D levels and from one patient suffering from X-linked hypophosphatemic rickets (Fig. 3). In both cases, we found the expected pathological increases of osteoid volume and thickness, albeit both parameters were significantly lower in the cases of vitamin D deficiency compared to adult hypophosphatasia. Most importantly, however, the number of osteoblasts was only elevated in individuals with adult hypophosphatasia, but not in individuals with vitamin D deficiency, and the same was

Fig. 3 Histomorphometric analysis of iliac crest biopsies derived from control individuals (CO) or from patients with adult hypophosphatasia (HP), vitamin D deficiency (VD) or X-linked hypophosphatemic rickets (XLH). Bars represent means ± SD, and asterisks indicate statistically significant differences (*p*<0.05) between two groups (*n*=8)



the case for the changes in trabecular number and separation (Fig. 3).

Bone mineral density distribution measurements by quantitative backscattered electron imaging

Since the histomorphometric analysis clearly confirmed that the major skeletal abnormality associated with an *ALPL* inactivation is a pathological impairment of matrix mineralization, we finally addressed the question whether the mineralized bone matrix in hypophosphatasia patients contains the same amount and distribution of calcium, when compared to the control biopsies. This was achieved by measuring the BMDD using quantitative backscattered electron microscopy. Here we found that the mineral distribution was indeed markedly impaired in sections from hypophosphatasia patients, with an increased amount of bone packets in a low mineralized state (Fig. 4a). In the hypophosphatasia sections, we further observed a reduction of bright pixels and a decrease of the mean gray value compared to the control cases, which is reflected by a significantly decreased overall calcium content (Ca mean wt). The significantly lower calcium width (Ca width wt) reflects a less heterogenic structure due to the absence of highly mineralized bone packages (Fig. 4b, c). Again, we performed the same measurements for the cases of vitamin D deficiency, but here we failed to detect a statistically significant difference compared to the control group. Interestingly, however, the overall calcium content (Ca mean wt) was decreased in the one case of X-linked hypophosphatemic rickets, representing the influence of *PHEX* inactivation on BMD, which needs to be confirmed in a larger number of affected individuals.

Discussion

Taken together, our study demonstrates that individuals suffering from adult hypophosphatasia display specific skeletal abnormalities, in addition to the previously established osteomalacia. These include increased trabecular number, decreased trabecular separation, as well as increased osteoblast number and surface compared to age-matched control individuals and compared to individuals with osteomalacia due to low circulating vitamin D levels. Moreover, we were able to show that the calcium content within the mineralized phase was significantly lower in the cases of hypophosphatasia, an aspect of the phenotype, which has not been addressed before. Although we can only speculate whether these previously unrecognized skeletal abnormalities contribute to the increased fracture rate observed in hypophosphatasia patients, we believe that our data are an important contribution to our understanding

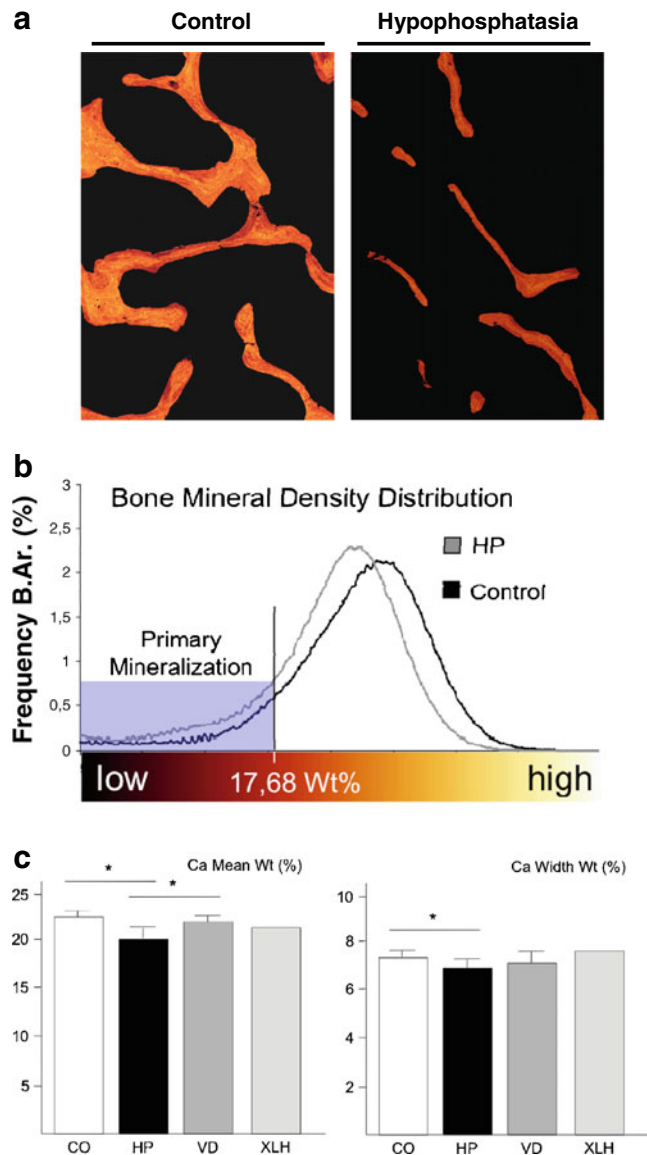


Fig. 4 Measurement of BMDD in non-decalcified bone biopsies from hypophosphatasia patients and control individuals. **a** Quantitative backscattered electron images expressed by pseudo-colors ($\times 25$ magnification). Highly mineralized bone is represented by *brightly colored pixels*, whereas lower mineralized bone areas are predominant in *darker colors*. Completely unmineralized tissue, such as the bone marrow, remains *black*. **b** The BMDD evaluated by the appropriate gray levels characterizes the mineralization profile of the hypophosphatasia patients (*gray graph*) and the control cases (*black graph*). The evaluated histogram revealed an increase of mineralized bone underlying primary mineralization in hypophosphatasia patients (mineralized bone beneath 17.68 wt.% Ca). **c** Quantification of the overall calcium content (Ca mean wt) and calcium width (Ca width wt) for control individuals (CO) or for patients with adult hypophosphatasia (HP), vitamin D deficiency (VD), or X-linked hypophosphatemic rickets (XLH). Bars represent means \pm SD, and *asterisks* indicate statistically significant differences ($p < 0.05$) between two groups ($n = 8$)

of this disease, especially since there are only few histomorphometric studies published so far [16, 21, 23–26].

The largest of these studies, involving 17 patients with adult hypophosphatasia, has been reported in 1984 [21], which was 3 years before the standardization of histomorphometric parameters by the American Society for Bone and Mineral Research [27]. However, although there are some structural histomorphometric parameters missing in this study, the authors have clearly demonstrated an accumulation of osteoid as the major abnormality. This osteomalacia was especially pronounced in the six individuals with a history of fractures (mean osteoid volume of 27.5%) and less evident in individuals only displaying altered serum parameters, which were mostly first-degree relatives of the above-mentioned individuals (mean osteoid volume of 4.5%). While there was no consistent change in the number of osteoblasts observed in this collective, it was interesting that the five cases, where no enrichment of osteoid has been observed, displayed histological features of low bone turnover, including a decrease of fluorescent labeling following tetracycline administration.

In this regard, we would like to point out that one major weakness of our study is that the patients did not receive tetracycline, thus excluding the possibility of dynamic histomorphometry. However, as in our study, all hypophosphatasia cases were characterized by a pathological accumulation of osteoid; we believe that it would have been difficult to demonstrate low bone turnover here, since in the case of osteomalacia, one can only observe diffuse tetracycline labeling, which cannot be utilized to determine the mineral apposition rate. Thus, it is probably most important that, besides the osteomalacia, we have found altered parameters of trabecular architecture, as well as increased numbers of osteoblasts, both of which have not been reported for the patients analyzed by Fallon et al. However, in one case of infantile hypophosphatasia, similar observations have been made [24]. In addition, our study has demonstrated for the first time that adult hypophosphatasia is not only characterized by an enrichment of non-mineralized osteoid, but also by impaired mineralization of non-osteoid areas, which may contribute to the detrimental effects of *ALPL* inactivation on skeletal stability.

Albeit interesting, however, our results certainly raise the question whether the observed abnormalities are unique to hypophosphatasia, or if they are also found in other forms of osteomalacia, such as vitamin D deficiency [41–43] or hypophosphatemic rickets [44, 45]. In an attempt to address this question, we have so far performed a histomorphometric analysis of iliac crest biopsies from eight individuals with low circulating levels of 25(OH)-vitamin D and from one individual suffering from X-linked hypophosphatemic rickets. While we did observe a low BMDD in the latter case, we found no significant differences between the

control and vitamin D deficiency cases by qBEI measurement. Moreover, both the increased and decreased trabecular separations were specifically observed in the cases of adult hypophosphatasia, and there was also no increased number of osteoblasts in the cases of vitamin D deficiency. Taken together, our findings have revealed some previously unrecognized skeletal alterations in adult hypophosphatasia patients, which are not generally observed in disorders with impaired skeletal mineralization.

Acknowledgments The authors thank Ms. Olga Winter for excellent technical assistance in preparing the samples for qualitative and quantitative histomorphometry.

Conflicts of interest None.

References

- Mornet E (2008) Hypophosphatasia. *Best Pract Res Clin Rheumatol* 22:113–127
- Greenberg CR, Evans JA, McKendry-Smith S, Redekopp S, Haworth JC, Mulivor R, Chodirker BN (1990) Infantile hypophosphatasia: localization within chromosome region 1p36.1-34 and prenatal diagnosis using linked DNA markers. *Am J Hum Genet* 46:286–292
- Henthorn PS, Raducha M, Fedde KN, Lafferty MA, Whyte MP (1992) Different missense mutations at the tissue-nonspecific alkaline phosphatase gene locus in autosomal recessively inherited forms of mild and severe hypophosphatasia. *Proc Natl Acad Sci USA* 89:9924–9928
- Henthorn PS, Whyte MP (1992) Missense mutations of the tissue-nonspecific alkaline phosphatase gene in hypophosphatasia. *Clin Chem* 38:2501–2505
- Moore CA, Ward JC, Rivas ML, Magill HL, Whyte MP (1990) Infantile hypophosphatasia: autosomal recessive transmission to two related sibships. *Am J Med Genet* 36:15–22
- Orimo H, Goseki-Sone M, Sato S, Shimada T (1997) Detection of deletion 1154–1156 hypophosphatasia mutation using TNSALP exon amplification. *Genomics* 42:364–366
- Orimo H, Hayashi Z, Watanabe A, Hirayama T, Shimada T (1994) Novel missense and frameshift mutations in the tissue-nonspecific alkaline phosphatase gene in a Japanese patient with hypophosphatasia. *Hum Mol Genet* 3:1683–1684
- Fauvert D, Brun-Heath I, Lia-Baldini AS, Bellazi L, Taillandier A, Serre JL, de Mazancourt P, Mornet E (2009) Mild forms of hypophosphatasia mostly result from dominant negative effect of severe alleles or from compound heterozygosity for severe and moderate alleles. *BMC Med Genet* 10:51
- Whyte MP, Wenkert D, McAlister WH, Mughal MZ, Freemont AJ, Whitehouse R, Baildam EM, Coburn SP, Ryan LM, Mumm S (2009) Chronic recurrent multifocal osteomyelitis mimicked in childhood hypophosphatasia. *J Bone Miner Res* 24:1493–1505
- Whyte MP (1990) Heritable metabolic and dysplastic bone diseases. *Endocrinol Metab Clin North Am* 19:133–173
- Brun-Heath I, Chabrol E, Fox M, Drexler K, Petit C, Taillandier A, De Mazancourt P, Serre JL, Mornet E (2008) A case of lethal hypophosphatasia providing new insights into the perinatal benign form of hypophosphatasia and expression of the *ALPL* gene. *Clin Genet* 73:245–250

12. Smilari P, Romeo DM, Palazzo P, Meli C, Sorge G (2005) Neonatal hypophosphatasia and seizures. A case report. *Minerva Pediatr* 57:319–323
13. Whyte MP (1995) Hypophosphatasia. In: Scriver CR, Beaudet AL, Sly WS, Valle D (eds) *The metabolic and molecular bases of inherited disease*. McGraw-Hill, New York, pp 4095–4112
14. Whyte MP (1994) Hypophosphatasia and the role of alkaline phosphatase in skeletal mineralization. *Endocr Rev* 15:439–461
15. Coe JD, Murphy WA, Whyte MP (1986) Management of femoral fractures and pseudofractures in adult hypophosphatasia. *J Bone Joint Surg Am* 68:981–990
16. Barvencik F, Gebauer M, Schinke T, Amling M (2008) Case report: multiple fractures in a patient with mutations of TWIST1 and TNSALP. *Clin Orthop Relat Res* 466:990–996
17. Reibel A, Maniere MC, Clauss F, Droz D, Alembik Y, Mornet E, Bloch-Zupan A (2009) Orofacial phenotype and genotype findings in all subtypes of hypophosphatasia. *Orphanet J Rare Dis* 4:6
18. Whyte MP (2009) Atypical femoral fractures, bisphosphonates, and adult hypophosphatasia. *J Bone Miner Res* 24:1132–1134
19. Mornet E (2007) Hypophosphatasia. *Orphanet J Rare Dis* 2:40
20. Mornet E (2010) The tissue nonspecific alkaline phosphatase gene mutations database. At http://www.sesep.uvsq.fr/03_hypo_mutations.php. Accessed 12 August 2010
21. Fallon MD, Teitelbaum SL, Weinstein RS, Goldfischer S, Brown DM, Whyte MP (1984) Hypophosphatasia: clinicopathologic comparison of the infantile, childhood, and adult forms. *Medicine (Baltimore)* 63:12–24
22. Ramage IJ, Howatson AJ, Beattie TJ (1996) Hypophosphatasia. *J Clin Pathol* 49:682–684
23. Ornoy A, Adomian GE, Rimoin DL (1985) Histologic and ultrastructural studies on the mineralization process in hypophosphatasia. *Am J Med Genet* 22:743–758
24. Wolff C, Zabransky S (1982) Hypophosphatasia congenita letalis. *Eur J Pediatr* 138:197–199
25. Anderson HC, Hsu HH, Morris DC, Fedde KN, Whyte MP (1997) Matrix vesicles in osteomalacic hypophosphatasia bone contain apatite-like mineral crystals. *Am J Pathol* 151:1555–1561
26. Whyte MP (2002) Hypophosphatasia. In: Bilezikian JP, Raisz LG, Rodan GA (eds) *Principles of bone biology*, 2nd edn. Academic, San Diego, pp 1129–1248
27. Parfitt AM, Drezner MK, Glorieux FH, Kanis JA, Malluche H, Meunier PJ, Ott SM, Recker RR (1987) Bone histomorphometry: standardization of nomenclature, symbols, and units. Report of the ASBMR Histomorphometry Nomenclature Committee. *J Bone Miner Res* 2:595–610
28. Bordier P (1972) Quantitative histology of metabolic bone disease. *J Clin Endocrinol Metab* 1:197–215
29. Amling M, Hahn M, Wening VJ, Grote HJ, Delling G (1994) The microarchitecture of the axis as the predisposing factor for fracture of the base of the odontoid process. A histomorphometric analysis of twenty-two autopsy specimens. *J Bone Joint Surg Am* 76:1840–1846
30. Amling M, Grote HJ, Posl M, Hahn M, Delling G (1994) Polyostotic heterogeneity of the spine in osteoporosis. Quantitative analysis and three-dimensional morphology. *Bone Miner* 27:193–208
31. Amling M, Herden S, Posl M, Hahn M, Ritzel H, Delling G (1996) Heterogeneity of the skeleton: comparison of the trabecular microarchitecture of the spine, the iliac crest, the femur, and the calcaneus. *J Bone Miner Res* 11:36–45
32. Amling M, Priemel M, Holzmann T, Chapin K, Rueger JM, Baron R, Demay MB (1999) Rescue of the skeletal phenotype of vitamin D receptor-ablated mice in the setting of normal mineral ion homeostasis: formal histomorphometric and biomechanical analyses. *Endocrinology* 140:4982–4987
33. Jones SJ, Glorieux FH, Travers R, Boyde A (1999) The microscopic structure of bone in normal children and patients with osteogenesis imperfecta: a survey using backscattered electron imaging. *Calcif Tissue Int* 64:8–17
34. Roschger P, Plenck HJ, Klaushofer K, Eschberger J (1995) A new scanning electron microscopy approach to the quantification of bone mineral distribution: backscattered electron image grey-levels correlated to calcium K alpha-line intensities. *Scan Microsc* 9:75–86
35. Roschger P, Paschalis EP, Fratzl P, Klaushofer K (2008) Bone mineralization density distribution in health and disease. *Bone* 42:456–466
36. Skedros JG, Bloebaum RD, Bachus KN, Boyce TM, Constantz B (1993) Influence of mineral content and composition on gray-levels in backscattered electron images of bone. *J Biomed Mater Res* 27:57–64
37. Boyde A, Maconnachie E, Reid SA, Delling G, Mundy GR (1986) Scanning electron microscopy in bone pathology: review of methods, potential and applications. *Scan Electron Microsc* 1537–1554
38. Boyde A, Travers R, Glorieux FH, Jones SJ (1999) The mineralization density of iliac crest bone from children with osteogenesis imperfecta. *Calcif Tissue Int* 64:185–190
39. Roschger P, Fratzl P, Eschberger J, Klaushofer K (1998) Validation of quantitative backscattered electron imaging for the measurement of mineral density distribution in human bone biopsies. *Bone* 23:319–326
40. Balena R, Shih MS, Parfitt AM (1992) Bone resorption and formation on the periosteal envelope of the ilium: a histomorphometric study in healthy women. *J Bone Miner Res* 7:1475–1482
41. Priemel M, von Domarus C, Klatte TO, Kessler S, Schlie J, Meier S, Proksch N, Pastor F, Netter C, Streichert T, Püschel K, Amling M (2010) Bone mineralization defects and vitamin D deficiency: histomorphometric analysis of iliac crest bone biopsies and circulating 25-hydroxyvitamin D in 675 patients. *J Bone Miner Res* 25:305–312
42. Liberman UA (2007) Vitamin D-resistant diseases. *J Bone Miner Res Suppl* 2:105–107
43. Koren R (2006) Vitamin D receptor defects: the story of hereditary resistance to vitamin D. *Pediatr Endocrinol Rev Suppl* 3:470–475
44. Beck-Nielsen SS, Brusgaard K, Rasmussen LM, Brixen K, Brock-Jacobsen B, Poulsen MR, Vestergaard P, Ralston SH, Albagha OM, Poulsen S, Haubek D, Gjørup H, Hintze H, Andersen MG, Heickendorff L, Hjelmborg J, Gram J (2010) Phenotype presentation of hypophosphatemic rickets in adults. *Calcif Tissue Int* 87:108–119
45. Imel EA, DiMeglio LA, Hui SL, Carpenter TO, Econs MJ (2010) Treatment of X-linked hypophosphatemia with calcitriol and phosphate increases circulating fibroblast growth factor 23 concentrations. *J Clin Endocrinol Metab* 95:1846–1850